Satellite-derived sea surface height and sea surface wind data fusion for spilled oil tracking

Kozai, Katsutoshi

(Citation)
Advances in Space Research,32(11):2287-2293

(Issue Date)
2003-12

(Resource Type)
journal article

(Version)
Accepted Manuscript

(URL)
https://hdl.handle.net/20.500.14094/90000003

SATELLITE-DERIVED SEA SURFACE HEIGHT AND SEA SURFACE WIND DATA FUSION FOR SPILLED OIL TRACKING

K.Kozai

Kobe University of Mercantile Marine, 5-1-1 Fukaeminami, Higashinada, Kobe 658-0022, Japan

ABSTRACT

An attempt is made to estimate the trajectory of spilled oil from the sunken tanker Nakhodka occurred in January 2, 1997 in Japan Sea by fusing two microwave sensor data, namely ERS-2 altimeter and ADEOS/NSCAT scatterometer data. In this study ‘fusion’ is defined as the method of more reliable prediction for the trajectory of spilled oil than before. Geostrophic current vectors are derived from ERS-2 altimeter and wind-induced drift vectors are derived from ADEOS/NSCAT scatterometer data. These two different satellite-derived vectors are 'fused' together in the surface current model to estimate and evaluate the trajectory of spilled oil from the sunken tanker Nakhodka. The distribution of component of spill vector is mostly accounted for by the distribution of geostrophic velocity component during the study period with some discrepancies during March, 1997.

INTRODUCTION

Data fusion is defined as a framework with the purpose of obtaining information of 'greater quality'. Within the framework tools are expressed for the alliance of data originating from different sources (Wald, 1999). For example the wavelet analysis and the scale functions are used for fusing the images with different spatial resolutions (Núñez et al., 1999, Ranchin and Wald, 2000). The exact definition of 'greater quality' is stated in this context as more reliable prediction for the trajectory of spilled oil from two different microwave sensor data, namely ERS-2 altimeter and ADEOS/NSCAT scatterometer data. An example is presented in the case of trajectory of spilled oil from the sunken tanker Nakhodka occurred in January 2, 1997 in Japan Sea. Geostrophic current vectors are derived from ERS-2 altimeter and wind-induced current vectors are derived from ADEOS/NSCAT scatterometer data. These two different satellite-derived vectors are 'fused' together in the surface current model to estimate and evaluate the trajectory of spilled oil from the sunken tanker Nakhodka.

DATA AND METHOD

Spilled oil accident made by the tanker Nakhodka in Jan.2, 1997 indicated the following characteristics. One is the spilled heavy oil with the bow section of the tanker drifted toward the coast of Japan Sea. The other is the continuation of oil spill from the sunken part of the tanker at the depth of 2500 meters more than a year. Figure 1 shows the Study area (132E-137E, 36N-40N) with two ERS-2 orbits (dotted lines, 270, 463). Cross and solid triangle indicate the locations of sunken tanker Nakhodka and the JMA buoy 21002, respectively. According to the press release from Maritime Safety Agency on the accident (1997), the locations and conditions around oil upwelling points are observed daily and spilled oil seems to be affected by the local winds and currents. Spilled oil has been monitored by various airborne and satellite sensors (NASDA, 1997). However the use of satellite remote sensing techniques are limited in each sensor and the optimal combination of satellite sensor for spilled oil are still under investigation. The purpose of the study is to propose an effective approach for tracking spilled oil by fusing the different satellite microwave sensor-derived vectors, namely geostrophic current vectors and wind-induced drift vectors.

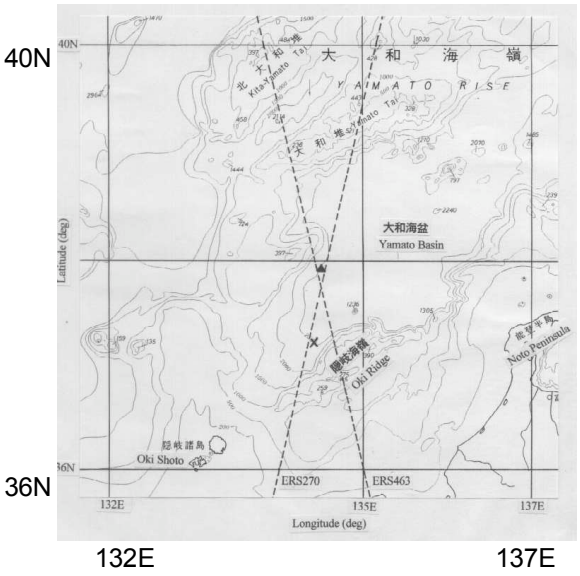

Fig. 1. Study area (132E-137E, 36N-40N) with two ERS-2 orbits (dotted lines, 270, 463). X and ▲ indicate the locations of sunken tanker Nakhodka and the JMA buoy 21002, respectively.

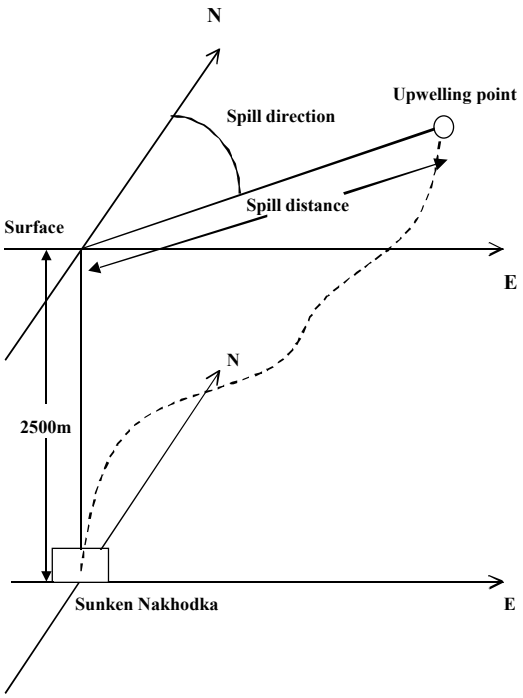

Fig. 2 Definition of spill direction and spill distance. □indicates the location of upwelling point at sea surface. Dotted line shows the estimated path of spilled oil from the sunken Nakhodka.

Oil upwelling points are characterized by the spill vector consisting of spill distance and direction. Spill distance is defined as a horizontal distance from the oil upwelling point to the location of sunken Nakhodka and a spill direction is defined as an angle made by the geographic north and the line corresponding to the spill distance shown in Figure 2. Figure 3 illustrates the temporal distribution of spill vector from Jan.17 to Apr.20, 1997. The locations of oil upwelling point are corresponding to the tip of each spill vector. It is found that eastward spill vectors are dominant until Julian Day 74 (Mar.15) and the westward spill vectors are frequently seen after March 15th. The maximum spill distance and direction are 4.7km, 288 degrees in Mar. 26 (Julian Day 85), 1997 respectively.

In order to monitor and track spilled oil from the sunken Nakhodka geostrophic current vectors derived from ERS-2 altimeter and wind-induced drift vectors derived from ADEOS/NSCAT scatterometer are fused together to estimate synthesized surface current vector. According to Ogura (1998), it is possible to predict the direction and distance of spilled oil based on the dominant wind vectors and the surface current vectors. In general the collinear method is used in order to calculate the dynamic sea surface height from the satellite altimeter data (Kuragano and Shibata, 1997). In this study the dynamic sea surface height is derived from the sum of the mean sea surface height from the model (GFDL MOM) (Hirose, 1999) and the temporal anomaly from the mean sea surface height from the ERS-2 altimeter data provided from NASA GSFC Ocean Pathfinder. Major specifications of ERS-2 altimeter are shown in Table 1. Figure 4 shows an example of the comparison of various sea surface heights along the orbit. According to Figure 4 sea surface heights expressed as the Anomaly+Mean increases toward south, which implies the stronger eastward geostrophic current in this region. From the dynamic sea surface height geostrophic current speed Vc can be calculated as follows (Strub, et al., 1997).

$$Vc(i)=\frac{g}{f}\frac{\partial h}{\partial s}=-\frac{g}{f}\left[\frac{h(i+n)-h(i-n)}{2n\Delta s}\right] \quad (1)$$

where Vc is the geostrophic current speed, g is the acceleration of gravity, f is the Coriolis parameter, h is the sea surface height, s is the vertical coordinate, i is the index of the coordinate grid point, and n is the half span of the centered difference. In this study a span of 14 intervals (n=7) is used to produce a 24km difference.

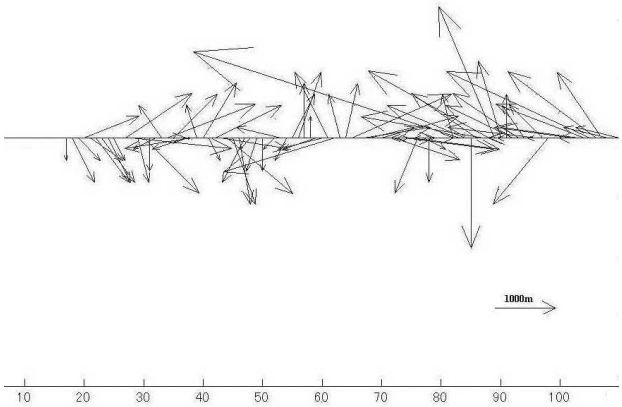

Fig. 3 Temporal distribution of spill vector from Julian Day 17 (Jan.17) to Julian Day 110 (Apr.20), 1997. (Horizontal coordinate shows the Julian Day.)

Table 1. Major specifications of ERS-2 altimeter.

Altitude	800km
Radar Frequency power	50w
Beam width	1.3 degrees
Footprint	1.7km
Pulse width	3 ns
Noise	4cm

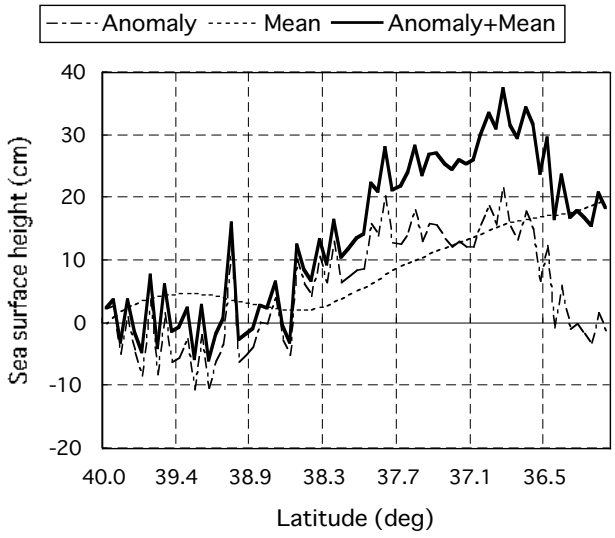

Fig.4 Comparison of various sea surface heights along the ERS-2 orbit 270. (Sea surface anomaly from the ERS-2 orbit 270, Jan.1, 1997, mean sea surface height simulated by the model (GFDL MOM) and the sum of anomaly and mean sea surface height.)

NSCAT is the abbreviation of NASA Scatterometer onboard ADEOS (Advanced Earth Observing Satellite) launched in 1996 and ceased its operation in June, 1997 because of the power failure of ADEOS. Major mission requirements of NSCAT are listed in Table 2. In this study W25 product with 25 km spatial resolution is used for the analysis. Since the W25 products along each orbit are not spatially gridded in terms of latitude and longitude, W25 products are resampled every 25km by using the nearest neighbor method (Lillesand and Kiefer, 2000). An example of wind vector distribution in Mar.25, 01h 56m (UT) is shown in Figure 5. Wind directions are mostly west and the wind speeds range from 11 to 15 m/sec. Based on the sea surface wind vectors available the wind-induced drift vectors are derived from the wind drift model. The wind drift model is defined as that the drift speed is 3% of the wind speed and the drift direction is 15 degrees to the right of the wind direction in the northern hemisphere (Espedal and Wahl, 1999). In order to evaluate the spilled oil trajectories the two different vectors namely geostrophic current vectors and the wind-induced drift vectors are fused as follows to estimate the synthesized surface current vector.

Synthesized surface current vector = geostrophic current vector + wind-induced drift vector (2)

RESULTS AND DISCUSSION

Based on the Eq.(1) above geostrophic velocity components along the ERS-2 altimeter orbit 270 and 463 are calculated and illustrated in Figure 6. It is found that the high velocity component region more than 20cm/sec is located along the 38 degree North throughout the study period. As far as the temporal distribution of velocity component at the location of sunken tanker (37.25 degrees North) is concerned, the eastward (positive) velocity component is indicated from the beginning to the Julian Day 40. However the westward (negative) velocity component is dominant during the rest of the period. These changes in velocity component are known to be closely associated with seasonal variability of sea surface temperature and anti-cyclonic eddy movement in the study area (Kozai, 1999). Figure 7 shows the result of comparison of geostrophic velocity components and east-west components of spill vector. Until the Julian Day 40 eastward (positive) velocity components are agreed well with eastward component of spill vector. On the other hand westward (negative) velocity components are corresponding well with westward components of spill vector throughout the rest of the period except the period of Julian Day from 63 to 80 (March, 1997). This means

Table 2 Major mission requirements of ADEOS/NSCAT

Wind speed	2m/s(rms) (for 3-20m/s)
Wind Direction	20deg.(rms) (for 3-30m/s)
Spatial Resolution	50km (Wind Cells)
Location Accuracy	25km(rms) (Absolute)
Coverage	90% of ocean every 2days

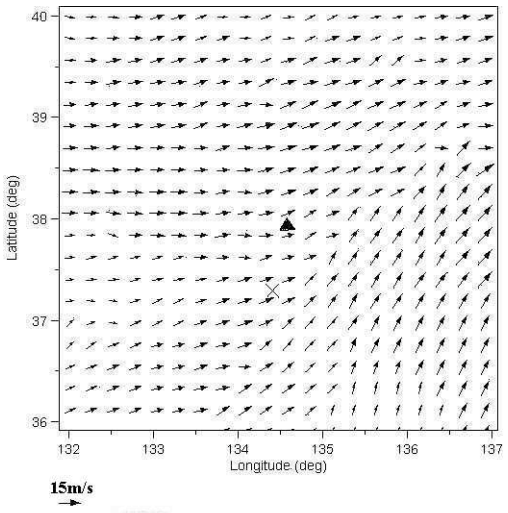

Fig. 5. Wind vector distribution derived from NSCAT (Mar.25, 01h56m(UT)). X and ▲ indicate the locations of sunken tanker Nakhodka and the JMA buoy 21002, respectively.

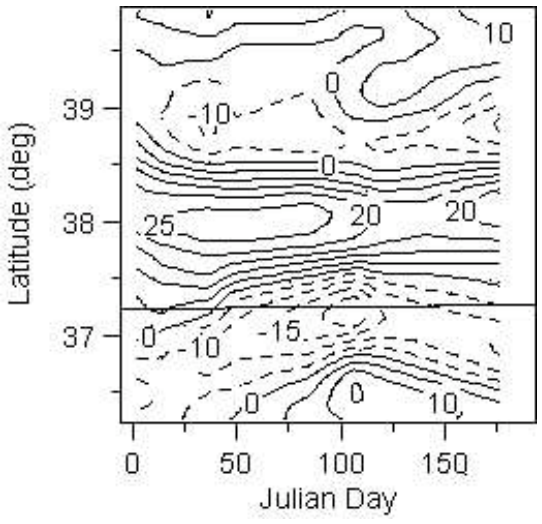

Fig. 6. Spatial and temporal distribution of geostrophic velocity component along the ERS-2 altimeter orbit 270 and 463. (Contour interval is 5cm/sec. Dotted lines indicate the contours below zero. Solid line shows the latitude of location of sunken tanker.)

that there must be some other factors (for example wind stress) interacting with surface flow for deviating the spill vectors while the distribution of component of spill vector is mostly explained by the distribution of geostrophic velocity component during the study period.

In order to account for the influence of wind vector on the surface flow the synthesized surface current vectors are calculated based on the Eq.(2) above and illustrated with NSCAT-derived wind vectors and spill vectors during March, 1997 in Figure 8. In the beginning half of the month NSCAT-derived wind speeds are generally higher than the one in the later half and the westerly wind directions are dominant, which generates eastward counter-flow to the westward geostrophic current. These conditions may lead to the shorter spill distance with unstable spill direction in the beginning half of the month in the spill vector distribution. On the other hand NSCAT-derived wind speeds are getting weaker in the later half while the geostrophic velocity components are getting stronger toward west shown in Figure 7. These conditions may be favorable to the geostrophic current which is accelerated by the wind-induced drift illustrated in Figure 9. Figure 9 shows the one of possible scenarios of different upwelling points before and after March 15, 1997 based on the results above. Before March 15 the geostrophic current vectors are decelerated or offset by the wind-induced drift caused by the westerly winds, which results in the shorter spill distance with unstable spill direction. After March 15 the geostrophic current

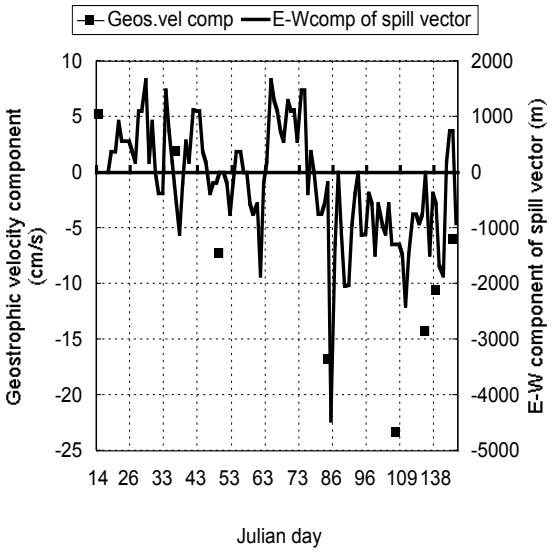

Fig. 7. Comparison of geostrophic velocity component and east-west component of spill vector.

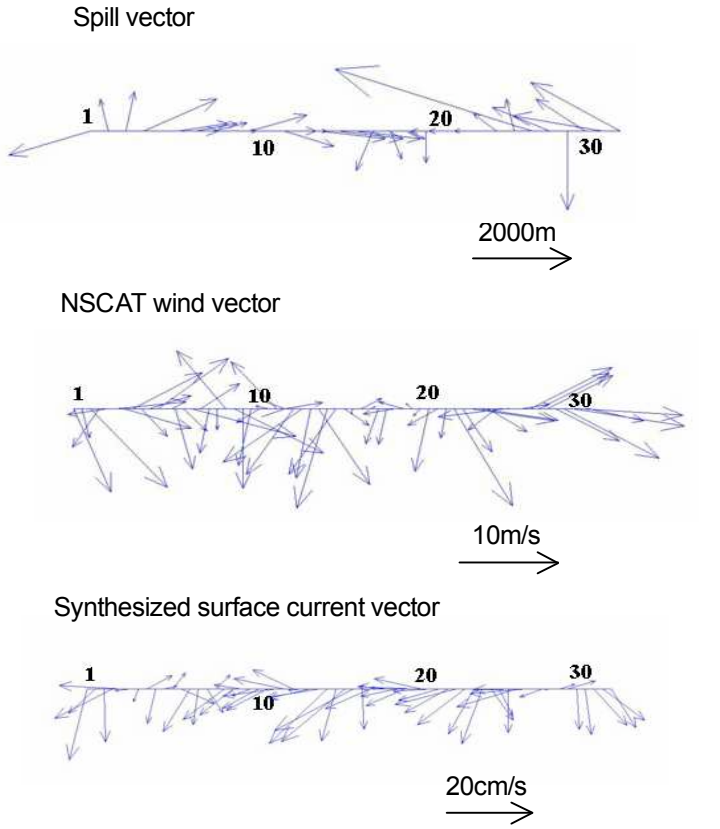

Fig. 8. Comparison of synthesized surface current vectors with spill vectors and NSCAT-derived wind vectors. (Numerals along the coordinate show the date in March, 1997.)

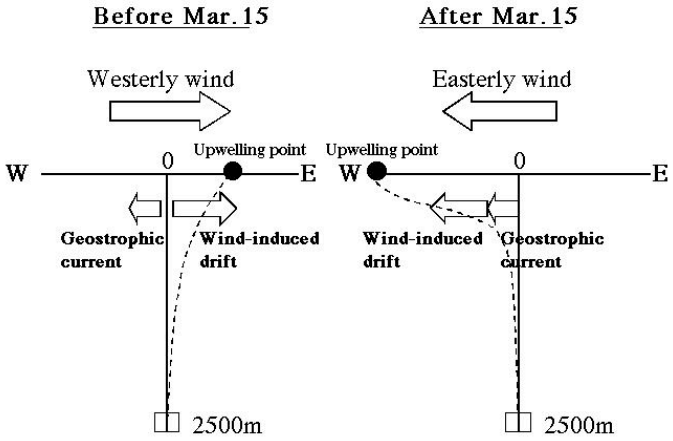

Fig. 9. Possible scenario of different upwelling points before and after Mar.,15, 1997.

vectors are accelerated by the wind-induced drift caused by the easterly winds, which results in the longer spill distance toward west.

While the scenario above is discussed only in the horizontal scale, it is highly probable that the distribution of spill vector is affected by the variability of internal structure of the ocean, for example the vertical velocity and density profile. In order to track effectively and accurately the spilled oil from the depth of 2500 meters it is inevitable to use the three dimensional advection-diffusion model with inputs of satellite-derived geostrophic current vectors and wind vectors.

SUMMARY

Results of the study are summarized as follows.

(1)Geostrophic current vectors and wind-induced drift vectors from two different satellite microwave sensors namely ERS-2 altimeter and ADEOS/NSCAT scatterometer are fused together for tracking spilled oil from 2500m depth in Japan Sea.

(2)The distribution of component of spill vector is mostly accounted for by the distribution of geostrophic velocity component during the study period with some discrepancies during March, 1997.

(3)Time series of synthesized surface current vectors in March, 1997 shows the two types of dominant pattern. One is that the geostrophic current vectors are accelerated by the wind-induced drift caused by the easterly wind, which results in the longer spill distance toward west. The other is that the geostrophic current vectors are decelerated or offset by the wind-induced drift caused by the westerly wind, which results in the shorter spill distance with unstable spill direction.

ACKNOWLEDGEMENTS

The author would like to acknowledge Mr.Higashiuwatoko, researcher in Remote Sensing Technology Center of Japan for providing ADEOS/NSCAT data. The author also would like to express sincere gratitude to the following institutions and individuals for their assistance in providing various datasets; Dr.Hirose of Kyushu University, the oceanographic department of Maizuru Marine Observatory, Japan Meteorological Agency, Maritime Safety Agency, NASA/JPL/PODAAC.

REFERENCES

Espedal, H.A. and T. Wahl, Satellite SAR oil spill detection using wind history information, INT. J. REMOTE SENSING, **20**, 1, 49-65, 1999.

Hirose, N., Assimilation of Satellite Altimeter Data with Circulation Models of the Japan Sea, Ph.D thesis, Kyushu University, 27-57, 1999.

Kozai, K., Variation of satellite-derived sea surface topography in the southern part of the Japan Sea including the drifting period of Nakhodka bow section, J. of the Marine Meteorological Society (UMI TO SORA), **75**, 2, 21-34, 1999. (original in Japanese)

Kuragano,T and A. Shibata, Sea Surface Dynamic Height of the Pacific Ocean Derived from TOPEX/POSEIDON Altimeter Data: Calculation Method and Accuracy, J. Oceanography, **53**, 6, 585-599, 1997.

Lillesand, T.M. and R.W.Kiefer, REMOTE SENSING AND IMAGE INTERPRETATION, John Wiley & Sons, Inc., 724p, 2000.

National Space Development Agency of Japan (NASDA) (ed.), Observation of spilled heavy oil from airborne and satellite sensors, A report of investigation by satellite remote sensing for the Nakhodka oil spill accident, 108p, 1997. (original in Japanese).

Núñez, J., X. Otazu, O. Fors, et al., Multiresolution-Based Image Fusion with Additive Wavelet Decomposition, IEEE TRANSACTION ON GEOSCIENCE AND REMOTE SENSING, **37**, 3, 1204-1211, 1999.

Maritime Safety Agency, On the accident of spilled heavy oil from the tanker Nakhodka, press release, February 27, 1997. (original in Japanese)

Ogura, S., Frontline in response to oil spill accident, Petroleum/Natural Gas Review, **11**, 104-117, 1998. (original in Japanese)

Ranchin, T. and L. Wald, Fusion of High Spatial and Spectral Resolution Images : The ARSIS Concept and Its Implementation, Photogrammetric Engineering and Remote Sensing, **66**, 1, 49-61, 2000.

Strub,T.P., Chereskin,T.K., Niiler,P.P., James,C. and Levine,M.D., Altimeter-derived variability of surface velocities in the California Current System, J.Geophys.Res., **102**, C6, 12727-12748, 1997.

Wald, L., Some Terms of Reference in Data Fusion, IEEE TRANSACTION ON GEOSCIENCE AND REMOTE SENSING, **37**, 3, 1190-1193, 1999.

E-mail address of K.Kozai kouzai@cc.kshosen.ac.jp